

# Analysis of LPG Engine PID Parameter Control of Transient Air-fuel Ration Based on Improved Elman Neural Network

Yao Jubiao

College of Environmental and Energy Engineering, Beijing University of Technology, Beijing100022, China;  
Beijing Vocational College of Electronic Science, Beijing100029, China  
Email: yaojubiao@yahoo.com.cn

Jiang Keyu

Dept. of Informatics, Fort Hays State University, KS 67601 - 4099, USA  
Email: keyujky@gmail.com

Yao Chaoyi

Southwest Jiaotong University, Chengdu 610031, China

**Abstract**—This paper puts forward one kind of air-fuel ration control method which integrates improved Elman neural network with normal PI control. It constructs a model of the single LPG electro-plating engine and simulation platform for air-fuel ration controlling with GT-Power software which seamless connect to Matlab/Simulink based on JL1P39FMB single cylinder engine and develop the electronic fuel-injected controller based on Intel MCS-96. It also constructs mini LPG electro-plating engine experiment system for air-fuel ration to the LPG Injection System and adopt the new inlet channel injection type of duty ratio controlling injector. Help the throttle percentage-rev- duty cycle pulse spectrum diagram after the calibration bench experiment for the best duty cycle of mini electronic LPG-injected under the steady working conditions. It predicts the air-fuel ration signals of nontransmission delay through the Elman neural network. The normal PI controller which deals with the predictive signals implements the concurrent control of air-fuel ration under transient conditions. The bench test and the simulation result indicate that the control methods have the strong adaptation, which can make the statism of air-fuel ration under transient conditions on  $\pm 5\%$ .

**Index Terms**—PID parameter Control, Air-fuel ration under transient, Elman Neural Network, Predictive control

## I. INTRODUCTION

LPG (Liquefied Petroleum Gas) electro-plating engine control the air-fuel ration accurately when the engine in the stability condition. But automobile-used LPG electro-plating engines are almost all in transient running among actual operating mode. Inflation-exhaust and gas backflow lead to the fluctuation range increasing of air-fuel ration when transient running. So most scholars devoted to

improve precision of air-fuel ration and reduce the calibration process work. The model-based control strategy and the intellectual control strategy based on neural network are the new focus in air-fuel ration controlling field at present.

The technology that combines the electronic fuel injection and the three-way catalyst has become the most effectively method to decrease the exhaust pollution of the gasoline engine in vehicle. However, the efficiency is influenced by air fuel ratio greatly. If the high efficiency is required (above 80%), the air fuel ratio needs to be controlled about 14.7, and the error needs to be held within the range of  $\pm 3.5\%$ [1]. The engines of vehicle in cities operating in the steady state and the transient state, which alter frequently. The measured air fuel ratio signal is delayed due to the case that the UEGO sensor is fixed in the exhaust pipe of the engine. When the engine operates in the steady state, the controlled results of the air fuel ratio can meet the requirement of the three-way catalyst; When operating in the transient state, the throttle position changes greatly, the fluctuating amplitude of the air fuel ratio in the cylinder increases, then the transportation delay of the air fuel ratio degrades the control quality. In order to avoid this deficiency, most of the researchers dedicated themselves to study on how to improve the control quality and to reduce the workload of calibration process, thus the control strategy based on model or neural network become new research focus at present [2,3].

First in the essay, the transportation characteristics of the air fuel ratio were analyzed. And then, a kind of air fuel ratio control strategy that combined the modified neural network and the traditional PI controller was put forward in this paper, in which the neural network was used to estimate the air fuel ratio signal without the transportation delay, while the traditional PI controller

The Youthful Scientific Fund of Beijing University of Technology (200500244); The Scientific Fund of Beijing Education Commission (KM200900002004)

was used to control the transient air fuel ratio by using the estimated signal. The model of a single cylinder engine was set up by using GT-Power; the model of the control system was set up by using Simulink. According to the characteristic that GT-Power can be linked with Matlab/Simulink seamlessly, the simulation model of the air fuel ratio control of the gasoline engine was set up by using the coupled technique between the two kinds of software[4]. On basis of this, air fuel ratio control strategy that combined the neural network and the traditional PI controller was studied.

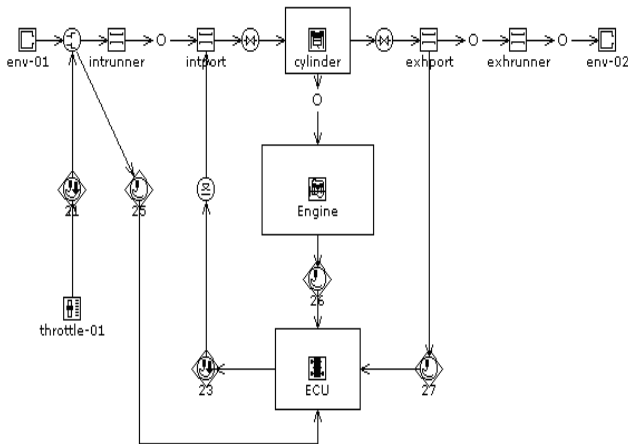


Figure 1. The model of a single cylinder electronic controlled gasoline engine

## II. ANALYSIS ON THE TRANSPORTATION CHARACTERISTICS OF AIR FUEL RATIO

### A. The duration $T_1$ of the mixture held inside the cylinders

The transportation delay of the air fuel ratio mainly includes the following three parts:

- 1)The duration  $T_1$  of the mixture held inside the cylinder.
- 2)The duration  $T_2$  of the waste gas flowing from the exhaust valve to the position of the UEGO sensor.
- 3)The response time  $T_3$  of the UEGO sensor.

The duration  $T_1$  is related to the rotate speed of the crankshaft, the crank angle from the closing of the intake valve to the opening of the exhaust valve, expressed as the following formula.

$$T_1 = \theta/6n \quad (1)$$

Herein,  $\theta$  denotes the crank angle while the mixture is held inside the cylinder in a working cycle,  $\theta = 360^\circ$  in this paper;  $n$  denotes the rotate speed of the crankshaft.

### B. The duration $T_2$ of the waste gas flowing from the exhaust valve to the position of UEGO sensor

The time  $T_2$  can be confirmed by the following formula [5]:

$$T_2 = V/v_{eg} \quad (2)$$

Herein,  $V$  denotes the cubage of the exhaust pipe, which is related to the structure of the exhaust pipe and

the position of UEGO sensor;  $v_{eg}$  denotes the volume velocity of the exhaust flow.

$$v_{eg} = (RT_{eg}/P_{eg}) \cdot \dot{m}_{eg} \quad (3)$$

Herein,  $R$  denotes the gas constant;  $T_{eg}$  denotes the temperature of the exhaust gas, which is related to the load of the engine;  $P_{eg}$  denotes the pressure of the exhaust pipe;  $\dot{m}_{eg}$  denotes the mass velocity of the flow.

### C. Set up the GT-Power model of enginer

Knowing from the working principle of the UEGO sensor, the value of the air fuel ratio is acquired by inspecting the electrical current of the pumped oxygen, so a certain response delay is in existence. It was supposed that the UEGO sensor belongs to a kind of apparatus with the first order response characteristic [6], the time constant was supposed at 100ms in this simulation .To the above analysis, the transportation delay of the air fuel ratio is related to the structural parameters of engines, operating condition of engines and the response characteristic of the UEGO sensor.

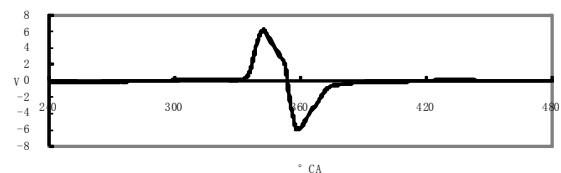


Figure 2. Trigger of magneto-ignition electrical fire

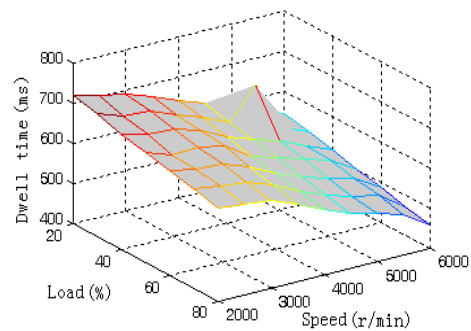


Figure 3. Calibration results on transmission delay of Air-fuel ration

Wave, Boost and GT-Power are popular one-dimensional engine simulation software at present. GT-Power is used most widely therein, which was adopted in this paper. The model of a single cylinder electronic controlled gasoline engine was set up in GT-Power, and the detailed structure is illustrated as Figure 1. The adjustable throttle valve was included in the model, whose adjustable range was 0~40mm. There was no intake pressure regulated cavity in the model, so the mass flow of the intake air was measured according to the throttle position and the rotate speed of the crankshaft. The input signals to the ECU included throttle position signal, crankshaft rotate speed signal and the feedback air fuel ratio signal, the output from the ECU was the

injection duration signal, the injection angle was set to 90° before the top dead-center, when the injection ended in a working cycle.

#### D. Accurate Comparison and Experiment Measurements

To provide an accurate comparison, measurements in all working condition should be consistent with the phase of engine working process. In this experiment, TDC is calibrated by CDI trigger signal which produced by engine magneto, and it will be regarded as the phase of the signal of recording measurements. The resolution of engine crank angle is 1°CA, and the maximum allowable speed is 12000r/min (instantaneous). The crank angle signal is used as the trigger signal, which is used to sampling once per degree of crank angle. The cylinder pressure signal and the TDC synchronization signal are recorded with the sampling frequency of 400 kHz. In order to ensure the integrality of information in sampling, there should be a sufficiently large sampling frequency in the system. Assuming that the maximum engine speed is  $n$ , and per degree crank angle can we get  $m$  sampling points, then the sampling frequency is:

$$f = \frac{n}{60} \times 360 \times m = 6mn(\text{Hz})$$

Data acquisition board uses the order sampling or synchronous acquisition time-transfer structure. If the maximum engine speed  $n = 9000\text{r/min}$ ,  $m = 1$ , channel = 2, the sampling frequency is required for the 108k. The system has the greatest sampling frequency 400k, fully meet the collection requirements. Angle encoder generates 3 signals, A, B, and Z. A, B signals mean that they can give a square wave signal for each degree of crank angle, and the phase distance is 1/4 degree of crank angle. A, B signals can be used to judge turning direction of crankshaft and raise the angle resolution to 0.25 degrees of the crank angle. Z signal is that it produces a square wave signal when the crank changes 360 degrees, which is used as the calibration TDC position synchronous signal in the acquisition system. In the measurement process, the angle encoder A signal is used as a trigger signal. It generates a square wave signal while crankshaft changes per angle, and the trigger sampling happens in the positive rising.

TABLE 1 CONTROL MODEL OF DUTY RATIO

Speed	idling	Small duty	med. duty	med. duty	full load	full load
1600	70%	75%	55%	30%	20%	10%
4500			45%	40%	35%	9%
6000			35%	35%	25%	5%

We can record the cylinder pressure and the TDC synchronization signal when the system sampling frequency comes to 400 kHz. The time difference is 2.5μs between the two signals, because it uses the order of

sampling. We use JL1P39FMB in the experiment. The maximum engine speed is 7200r/min, and the shortest time when the crankshaft changes per angle is 23μs, that is, synchronous signal TDC is behind the pressure signal at the time of maximum of about 0.1 crank angles. This error value is not heavy, and it can be eliminated by amend thermodynamics of TDC position.

Due to the big vibration and electromagnetic interference in the working environment of measure, the cylinder pressure signal and the angle coder signal will be impacted. In order to reduce this impact, we make use of shielded cable for all signal transmission in this system, and the entire system is commonly grounded to improve the anti-interference ability.

Top Dead Center (TDC) determination: It is very important to calibrate TDC accurately in the analysis. Usually when the maximum outburst pressure point in the cylinder reaches at 12~15° Crank Angle (CA) after TDC, the engine gets the best power and economy performance [7,8].

In this system, TDC is determined by the method of thermodynamic amendment on the maximum dragging compression pressure. Therefore, as long as the fixed difference between the position of angle coder synchronization signal and that of maximum dragging compression pressure is determined, then the position of TDC will be determined according to the location of sync signal.

Considering the angle coder may not be able to be installed, and in order to determine the approximate location of TDC, we have measured the trigger signal, which is emanated by engine magneto, of CDI non-contact ignition system in experiment, which is shown in Figure 2.

When trigger device rotates over trigger coil, magneto inducts the positive and negative pulse signal (which is shown in figure 2) to control the ignition time. The minimum value of negative pulse trigger signal corresponds to the position of TDC. In this way, TDC still can be calibrated even without angle coder. Sampling process: it needs large amounts of high-speedily and continuously sampled data in one measure. At the beginning, the acquisition card works according to the set method and rate of sampling.

Data are accessed to the on-board cache of 4K FIFO in time and channel order; when on-board FIFO has read into 2K data(half full), the interruption is generated, then 2048 data are written into the 2MB data buffer of computer. As the priority of interruption is higher than that of other operations, the function of saving data and displaying can be completed at the same time without affecting the integrity of the date that are read into the memory buffer.

### III. METHODS OF CALIBRATION EXPERIMENT

Calibration experiment is carried out in a LPG single-cylinder motorcycle engine with EFI. As a result of the adoption of LPG fuel supply mode with gaseity injection in gas inlet port, fuel film effect is not taken account of in calibration. In order to reduce the accumulation errors,

when calibrating transmission delay time of the air-fuel ratio, we consider the three stages of transmission delay of air-fuel ratio as a whole. Calibration experiment is carried out in steady-state condition; the specific experimental system is described as following. Engine fuel injection pulse width signal is a superposition of steady-state injection pulse width signal and disturbance signal. The steady-state pulse-width signal is exported by the ECU of LPG EFI engine according to the actual condition and the expected air-fuel ratio, while the disturbance signal is exported from D/A output channels which are embedded in AC6111 high-speed data acquisition card. We introduce AFRT as AFR disturbance and AFRe as AFR disturbance in exhaust, and then we record the changes over time of these two AFR disturbances. By comparing the phase difference between them we can measure transmission time of AFR. The outputs of engine intake manifold pressure sensor and air-fuel ratio sensor are connected respectively to the A/D channel embedded in AC6111 high-speed data acquisition card.

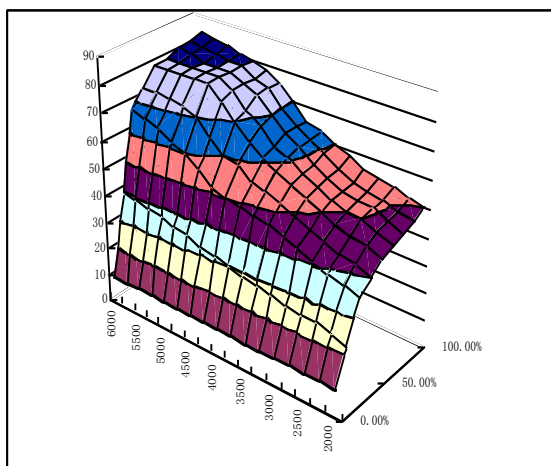


Figure 4. Duty-ratio control diagram

During the calibration experiments, we regulate DC power dynamometer and engine throttle. When the throttle position and speed are adjusted to working conditions that we want to calibrate, PC produces a positive salutation disturbance signal, which adds to steady injection pulse width signal, through the D/A channel embedded in AC6111. At the same time, PC

makes a high-speed sampling to the intake manifold pressure sensor (MAP) and air-fuel ratio sensor (UEGO). As a result of the speed-lock function of experimental DC power dynamometer, the disturbed speed can still be maintained at the calibrated speed point, while the air-fuel ratio sensor output will have a salutation. After analyzing the relationship between amplitude and phase of intake manifold pressure signal and those of air-fuel ratio signal, we can get the transmission time from intake valve closing, combustion and gas exhausting to the output of air-fuel ratio sensor in the calibrated working condition [9].

A. Construction of mathematical model and parameters optimized for Calibration Rresults

The operating condition variety scope of calibration experiment shows as follows: load from 20% to 80%, by the step 10%; Speed from 2000rpm to 6000rpm, by 500rpm step. The changes in the pulse spectrum of calibration results is illustrated in Figure 3, which shows that the air-fuel ratio transmission delay time is the function of the load and speed, with inverse proportion[10].

The experimental data under the low fuel consumption, low HC and CO emissions, and constrained NOX emissions are optimized on condition that the engine operates in security and stability. We choose the best results as the MAP basic raw data, which consider as the basic control data in different speed and throttle opening. The mathematical model is set by tabular method, zoned by the throttle position and speed. We compare the speed characteristics in a variety of throttle opening via the engine bench test to determine the optimum electric control parameters, which are put into the computer memory. The more detailed form, the smaller region formed by throttle and speed, and the higher control accuracy. However, because of restrictions on the sensor characteristics, throttle position is divided into six sections, which results discontinuous of the control volume in different regions, and makes the air-fuel ratio control a step change. Thus, interpolation table should be used in the actual control. The control model of duty ratio is shown in Table 1

B. Calibration results of duty-ratio control values

Duty-ratio control values are showed on Table2, and.

TABLE 2 DUTY-RATIO CONTROL VALUES

F	200			275		32	350					47				575	600
n	0	2250	2500	0	3000	50	0	3750	4000	4250	4500	50	5000	5250	5500	0	0
0	10	10	10	10	10	10	10	10	10	10	10	10	10	10	10	10	10
12.5%	22	24	25	25	26	27	28	29	30	31	32	35	35	37	38	39	39
25%	36	37	39	41	43	45	47	48	49	50	52	56	60	62	65	66	68
37.5%	40	42	43	45	47	49	52	54	55	59	60	65	70	72	73	74	74
50%	43	45	46	48	50	53	56	58	61	65	70	75	80	80	80	80	80
62.5%	45	47	50	50	52	54	57	61	63	68	72	77	80	80	80	80	80
75%	46	48	51	51	52	55	58	62	65	70	75	77	80	80	80	81	82
87.5%	48	49	51	52	53	56	59	62	65	70	75	77	80	80	81	82	83
100%	50	51	53	54	55	58	60	63	65	70	75	78	80	81	82	83	84

the Figure 4 is the duty-ratio control diagram above the duty-ratio control values.

IV. DIGITAL IMPLEMENTATION ON ALGORITHM OF PID

PID control based on the deviation calculates of the importation according to the proportion, integral and differential. The results of operation are exported as a control. PID control system for the basic structure program consists of the feedback principle, which is shown in Figure 5.

A. Analysis of the results of operation

Output  $c(t)$  is fed back to the input, then digital PID control is added by the deviation resulted in the comparison between the input signal and the feedback signal to regulate the volume  $u(t)$ , which is exported to the controlled plant. PID control adjusts the control volume according to the changes of deviation, and it is also known as digital PID regulator. For example, the deviation increases, and the control volume of  $u$  have also increased, which is proportional control. As the deviation  $E$  exists all the time, we should be integral, and the

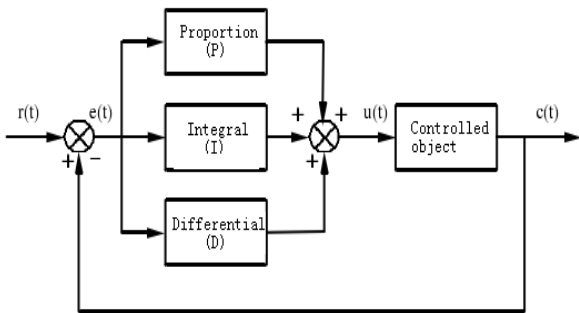


Figure 5. Elements of PID

Control volume is increasing to eliminate deviation  $E$ . This is called integral control. The differential control is expected to play the role, that is, when  $E > 0$ , indicating that the deviation is increasing, the control volume should be increased to reduce the deviation; When  $E < 0$  indicating that the deviation in reduction, the control volume should be reduced to avoid oscillation which is caused by deviation  $E$  developing in opposite direction when it trends to zero.

In practical applications, the structure of PID can be changed flexibly in accordance with the characteristics of the object and control requirements. Some parts of PID, such as proportion (P) regulation, proportion-integral (PI) regulation, proportion-integral-differential (PID), etc., can be taken to compose control rules. Especially in the computer control system, they can be more flexibly used, in order to give full play to the role of the computer.

In stimulation system, the formula of PID can be written as follow:

$$P(t) = K_p \left[ e(t) + \frac{1}{T_i} \int e(t)dt + T_d \frac{de(t)}{dt} \right] \quad (4)$$

In this formula,  $P(t)$ -output signal of regulator;  $e(t)$ -the deviation signal of regulator, which is equal to the error between the measured value and the given value;

$K_p$ -the proportion coefficient of regulator;

$T_i$ -the integral time of regulator;

$T_d$ -the differential time of regulator.

Because computer control is based on sampling control, which can only calculate the control volume by the deviation of the sampling time, firstly the formula (4) must be dispersed in computer control system. The differential equations for the system are replaced by the differential equations in digital form, in this way the integral parts can be expressed in the form of sum and increment:

$$P(t) = K_p \left[ e(t) + \frac{1}{T_i} \int e(t)dt + T_d \frac{de(t)}{dt} \right] \quad (5)$$

$$\frac{de(t)}{dt} \approx \frac{E(k) - E(k-1)}{\Delta t} = \frac{E(k) - E(k-1)}{T} \quad (6)$$

After putting the formula (5) and the formula (6) into the formula (4), we can get discrete PID expression:

$$P(k) = K_p \left\{ E(k) + \frac{T}{T_i} \sum_{j=0}^k E(j) + \frac{T_d}{T} [E(k) - E(k-1)] \right\} \quad (7)$$

In this formula,  $\Delta t = T$ -sampling period,  $T$  must be small enough to ensure a certain degree of accuracy;

$E(k)$ -the error at the time of  $k$ -sampling;

$E(k-1)$ -the error at the time of  $(k-1)$ -sampling;

$K$ -sampling number,  $k = 0, 1, 2, \dots$ ;

$P(k)$ -the output of the regulator at the time of  $k$ -sampling.

The output value of formula (7) corresponds with the opening position of the injector valve, therefore, usually formula (7) is called as the location formula for location-based PID control. It can be seen from formula(7), that if we want to calculate  $P(k)$ , we not only need the last error signal  $E(k)$  and current error signal  $E(k-1)$ , but also need to add the previous error signals  $E(j)$  for integral parts, that is,

$$\sum_{j=0}^k E(j)$$

In this way, not only the amount of calculation is huge, but also a large number of memory will be used to preserve  $E(j)$ . Thus, it is not convenient to control directly by formula(7). In order to solve this problem, we make following changes. According to the principle of recursion, the expression for output of PID at level  $(k-1)$  can be written as follow:

$$P(k-1) = K_p \left\{ E(k-1) + \frac{T}{T_i} \sum_{j=0}^{k-1} E(j) + \frac{T_d}{T} [E(k-1) - E(k-2)] \right\} \quad (8)$$

Formula(7)subtracted by formula(8),then get

$$P(k) = P(k-1) + K_p [E(k) - E(k-1)] + K_i E(k) + K_d [E(k) - 2E(k-1) + E(k-2)] \quad (9)$$

$$K_i = K_p \frac{T}{T_i}$$

is the integral action coefficient;

$$K_D = K_p \frac{T_D}{T}$$

is the differential coefficient.

From the formula(9), we can see that there is no need but to get the value of P(k-1), E(k), E(k-1) and E(k-2) to calculate the output value of P(k) at level k, so it is much simpler than the use of formula(7). In many control system, as actuating devices are controlled by step motor or multi-coil potentiometer, an incremental signal is enough. Therefore, by the formula (7) subtracted from formula (8), we can get:

$$\Delta P(k) = P(k) - P(k-1) = K_p [E(k) - E(k-1)] + K_I E(k) + K_D [E(k) - 2E(k-1) + E(k-2)] \quad (10)$$

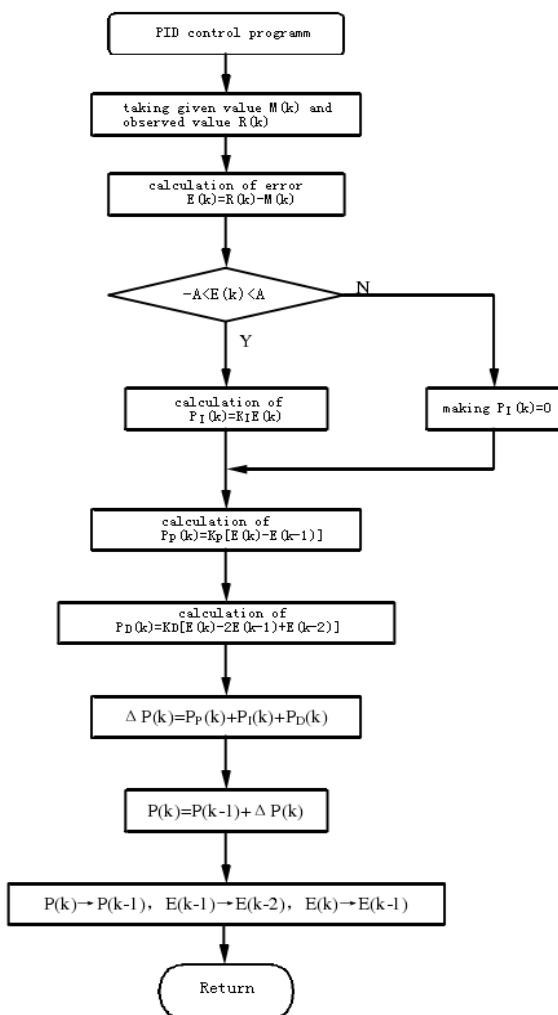


Figure 6. Flow chart of PID

The formula (10) shows that the increment of output at level k ( $\Delta P(k)$ ) is equivalent to the error between the output of regulator at level k and that at level k-1, that is, the increased (or decreased) value at level k-1. Therefore, formula (10) is called as the incremental PID controlling formula. In the position controlling formula, because of the total output, each output is relative to the original location. Therefore, not only E (j) needs to be cumulated,

but also any failure of computer will lead to a big change of P(k). Although the modifications of the incremental control are not so big, it has brought a lot of advantages: the impact of malfunction is small because of the incremental output in computer, if necessary, it can be removed by logic; in the position controlling algorithm, in order to achieve manual/automatic switch without disturbance, when the manual mode is being switched to the automatic mode, the output value of computer must be first of all equivalent to the original valve opening, that is,  $P(k-1)$ , which would creates difficulties for program design. In the incremental design, the output only is related to the error, not the original position of the injector valve. Thus the incremental algorithm is easy to achieve manual/automatic switch without disturbance, and as it doesn't create any uncontrolled integral, good regulating effects can be achieved easily.

However, this control also has its deficiencies: large integral truncation effects, which result in static error; large effects of overflow. Therefore, the right controlling algorithm should be chosen based on the actual situation of the object. Generally speaking, location-based algorithm should be adopted in the system that uses servo motor or thyristor as implementation device, or that has high requirement for controlling precision, while incremental algorithm should be adopted in the system that uses the step motor or multi-coil potentiometer as implementation device.

In addition to these two controlling algorithms, there is also another control algorithm which is called speed controlling algorithm. That is,

$$V(k) = \frac{\Delta P(k)}{T} = \frac{K_p}{T} \left\{ E(k) - E(k-1) + \frac{T}{T_I} E(k) + \frac{T_D}{T} [E(k) - 2E(k-1) + E(k-2)] \right\} \quad (11)$$

Discrete programming expression for the incremental PID algorithm from formula (10) can get the incremental PID algorithm as following:

$$\Delta P(k) = K_p [E(k) - E(k-1)] + K_I E(k) + K_D [E(k) - 2E(k-1) + E(k-2)]$$

So

$$P_p(k) = K_p [E(k) - E(k-1)]$$

$$P_I(k) = K_I E(k)$$

$$P_D(k) = K_D [E(k) - 2E(k-1) + E(k-2)]$$

And get

$$\Delta P(k) = P_p(k) + P_I(k) + P_D(k) \quad (12)$$

Formula (12) is the discrete programming expression for the incremental PID algorithm. It will be stored at the designated unit of RAM separately when get KP.KI.KD.

**B. Eliminates for PID controls**

In the general control of the PID regulator, because the linear range of the actuator is limited, when the deviation E become larger, such as system starting, stopping or significantly changing, because of the role of integral term, there will be a great overshoot leading to the system continual oscillation. This phenomenon affects more deeply the objects that change slow, such as temperature, liquid level -conditioning systems, and it also exists in the general simulation-conditioning systems. In order to eliminate this phenomenon in the computer control system, we can use the method of integration separation. That is, when the deviation exceeds a given range, integration does not work until the volume is adjusted to the given value. For the given value of R (k), measured value of M (k), the maximum allowable deviation value of A. The formula of separation control is shown as follows:

$$E(k) = |R(k) - M(k)| \begin{cases} > A, \text{ PD} \\ \leq A, \text{ PID} \end{cases} \quad (13)$$

By the use of integral action separation, the overshoot of controlled variable and the transition time can be reduced significantly, which improves the regulating performance.

PID control flow chart for the system with integral action separation, which is shown in Figure 6. In the initialization program, E (k-1), E (k-2), P (k-1) should be unit reset.

**V. DIGITAL CONTROL SYSTEM OF PID PARAMETERS**

Tuning parameters is very important in the digital control system, which impacts on the quality of regulation directly. PID control parameters include the sampling period T, the ratio of coefficient KP, integration time TI and the differential time TD. A reasonable choice of these parameters is one of the key issues in digital control system.

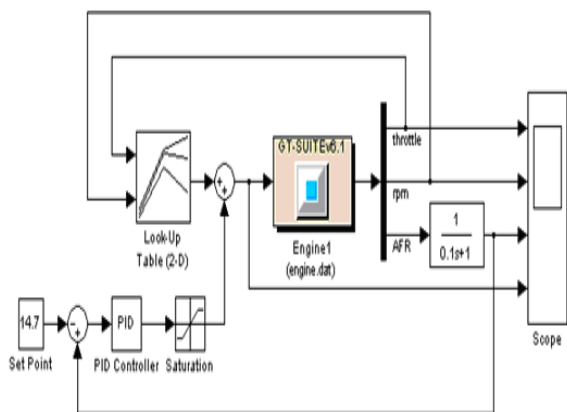


**Figure 7. The simulation model of air fuel ratio control with traditional PI controller**

Determination of sampling period T: according to the Shannon sampling theorem, fs stands the upper limit of the sampling frequency. If  $f_s \geq 2f_{max}$ , the system can be truly restored to the original continuous signal.

**A. The factors of impacting of sampling period**

By theory, the higher the sampling frequency, the smaller the distortion. However, from the controller itself, it adjust rely on deviation signal E (k). When the sampling period T is too small, the deviation signal E (k) will be too small, while the regulator will lose the function of adjustment. But sampling period T is too long, will cause the error. Therefore, the sampling period T must be considered synthetically.

The factors of impacting of sampling period T is described as follows: the higher disturbances frequency adding to the object, the higher sampling frequency, that is, sampling period is shorten; The dynamic characteristics of objects mainly connect with the object for the delay time  $\theta$  and time constant  $\tau$ , and when a significant delay time comes up, the sampling period T is basically the same with the pure delay time  $\theta$ ; If the digital control uses Dahlin algorithm and peninsula actuator, sampling period becomes longer; If digital control use the fastest non-corrugated systems stepper motors, sampling period become shorter; The larger the number of control loop, the longer the T, otherwise, we have smaller T; In general, the higher the control accuracy, the shorter the sampling period to reduce the time delay system .

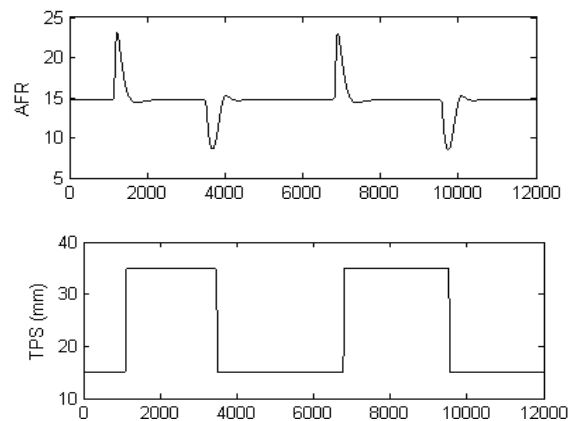


**Figure 8. The controlled results of air fuel ratio based on traditional PI controller**

There are two types of selection of sampling period, one is the calculation method, and the other is the experience method. Calculation is less used, because it is more complex, especially difficult to determine the constant time in every sectors of the controlled system. So-called experience is a multi-try method. That is, in accordance to the practice of working people, as well as the characteristics of the objects and parameters, we choose an approximate sampling period T firstly, putting it into the computer control system to test, and then we



repeat amendments to T until satisfied. Taking into account of the above factors, combined with the actual situation of the system, the sampling frequency take 10Hz, that is, sampling period  $T = 0.1s$ .

The selection of KP, TI, TD: Because of the process of actual control complexity and the changing parameters, it is difficult to determine the dynamic characteristics of plants. Sometimes, maybe you can find it, but in this way, not only it has the trouble in calculation and heavy workload, but also it has the big difference between the results and the actual value[11]. Therefore, the experience method is the most widely used. According to the specific

Regulating and the different characteristics of the object, after the closed-loop testing, we try it over and over to find the best adjustments.

For the specific circumstances of this system, because of the general adjustment of the injection of no more than the basic injection amount of 5% duty cycle, the adjustment of PID control of the duty ratio should not exceed 1%. Through the calibration of oxygen sensor, we consider the air-fuel ratio which correspond oxygen sensor output voltage of 0.5V as the theoretic air-fuel ratio.

So at last get  $KP = 0.005 = 1/200$ ,  $TI = 3.5$ ,  $TD = 1s$  and

$$K_I = K_p \frac{T}{T_I} = 1/7000$$

$$K_D = K_p \frac{T_D}{T} = 0.05 = 1/20$$

After packing the model in GT-Power, which is shown in Figure 1, it could be used for Simulink. The simulation model of air fuel ratio control with traditional PI controller is illustrated as Figure7, the injection duration signal input to the ECU was the sum of two parts: one was the look-up value according to the value of the throttle position and the crankshaft rotate speed, which needs to be calibrated in advance; the other was the calculated value of the PI controller according to the feedback from the UEGO sensor. The target value of the air fuel ratio was set to 14.7.

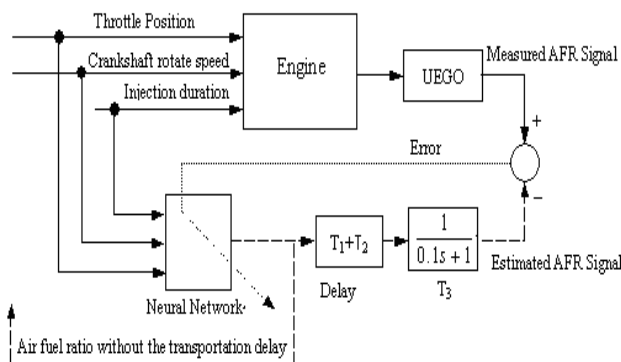


Figure 9. The simulation model of air fuel ratio control based on neural network

When the engine works in steady state, the air-fuel ratio can be controlled stably around the target value shown in Figure 8. When the engine works in transition condition, as a result of the "Charge Reflux" in intake

manifold and the transmission delay of air-fuel ratio, the air-fuel ratio will be down when throttle angle increasing, that is, the concentration of mixture will become higher when throttle angle decreasing.

C. Prediction method of the air fuel ratio without the transportation delay

For the forecast mode of air-fuel ratio without transportation delay, please refer to Figure 9.

The essence of the air fuel ratio is to control the mixture's concentration inside the cylinder, the perfect mode is to measure the mixture concentration inside the cylinder directly, and however the UEGO sensor can only be fixed in the exhaust pipe at present. In order to avoid the maladjustment of the air fuel ratio because of the transportation delay measured by the UEGO sensor, the assumption, which utilizes the air fuel ratio signal without the transportation delay to close the PI feedback controller, was put forward in this paper. The air fuel ratio without the transportation delay must be predicted, the prediction method is illustrated as Figure 9.

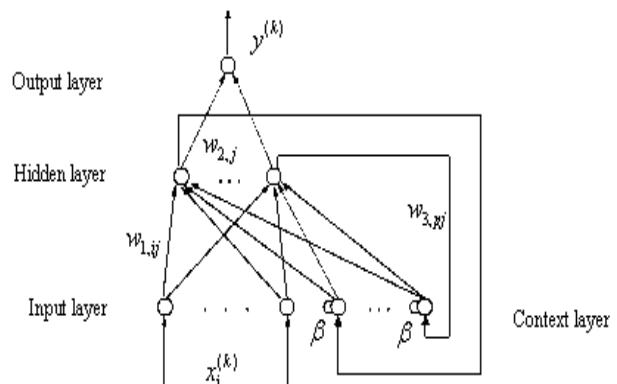


Figure10. The structure of the modified Elman neural network

From the fore mentioned analysis on the transportation delay of the air fuel ratio, T1, T2 and T3 can cause a bad quality of the air fuel ratio control. The air fuel ratio without the transportation delay can be acquired by training the neural network with the teacher's supervision on-line. Illustrated as Figure 9, the input to the neural network consists of throttle position signal, crankshaft rotate speed signal and the injection duration signal, the output from it was compared with the output of the UEGO sensor after being delayed by the T1, T2 and T3, then the training algorithm regulated the weight of each neuron in the neural network according to the compared error. The output from the neural network can be regarded as the air fuel ratio without the transportation delay when the error was limited within the set range. The transient air fuel ratio would be controlled perfectly when the trained signal acted as the feedback signal of the PI controller [12].

The air fuel ratio signal was taken from the exhaust valve in this simulation study, for sake of simplifying the model. So T2=0, only T1 and T3 were considered while the neural network is being trained.



The essential of air-fuel ratio control is controlling the concentration of air and fuel mixture, which is involved in the combustion. The ideal control mode is monitoring the concentration of in-cylinder mixed gas directly, but current air-fuel ratio sensor can only be installed in the exhaust manifold. In order to avoid the problem of maladjusted control to air-fuel ratio in transition condition caused by transmission delay, in this paper, the idea of air-fuel ratio prediction with no delay in transmission is proposed, which is shown in Figure 9. From foregoing analysis of transmission delay of air-fuel ratio, we can see that T1, the in-cylinder residence time of gas mixture after the closure of intake valve, and T2, the time that emission gas moves from exhaust valve to sensor, and T3, the response time of air-fuel ratio sensor, are the key effects on real-time control of air-fuel ratio. Therefore, we can realize the forecast of air-fuel ratio signal with no transmission delay by the use of supervised neural network learning. The input of neural network is the signal of throttle angle, speed signal and fuel injection pulse width value. After delayed by T1, T2 and T3, the output is compared to that of air-fuel ratio sensor. The error from the compare will be regarded as the basis of regulating neurons weight vector in neural network. When the error is controlled within the set range, the neural network output signal is the air-fuel ratio signal with no transmission delay. By using this signal as PID controller feedback signal, the real-time control of the air-fuel ratio in transition condition can be realized.

In this study, in order to simplify the model, air-fuel ratio signal is taken directly from the exhaust valve. So T2 = 0. Only T1 and T3 are taken account of when we delay on the output signal of neural networks.

## VI. THE STRUCTURE OF THE MODIFIED ELMAN NEURAL NETWORK

The modified Elman network adds the self-feedback connection in the context layer. It has been proven that the modified Elman network is efficient to identify the higher order system dynamically [5]. The self-feedback connections at the context layer simplify the dimensions of the network, and then the nonlinear model with higher precision could be acquired, using fewer neurons. So the modified Elman network is fit to the embed control system.

### A. Algorithm of the Modified Elman network

The modified Elman network can be regarded as a BP network with local mnemon and local feedback connection; its basic structure is illustrated as Figure 10. The modified Elman network consists of the input layer, the hidden layer, the context layer and the output layer. Each node in the hidden layer links with a corresponding node in the context layer, respectively. The nodes between the input layer and the hidden layer link with each other through adjustable weights, so do the nodes in the hidden layer and the output layer, the context layer and the hidden layer. There are self-feedback connections with the fixed gain  $\beta$  at the neurons in the context layer.

Suppose  $i$  denotes the nodes in the input layer,  $i = 1, \dots, M$ ,  $j$  denotes the nodes in the hidden layer,  $j = 1, \dots, L$ , and  $p$  denotes the nodes in the context layer,  $p = 1, \dots, L$ , then the connection weight from  $i$  to  $j$  can be denoted with  $w_{1,ij}$ , the connection weight from  $j$  to output layer can be denoted with  $w_{2,j}$ , and the connection weight from  $p$  to  $j$  can be denoted with  $w_{3,pj}$ ;  $net\_h_j$  denotes the input to node  $j$  in the hidden layer,  $o\_h_j$  denotes the output of node  $j$  in the hidden layer,  $net\_c_p$  denotes the input to node  $p$  in the context layer,  $o\_c_p$  denotes the output of node  $p$  in the hidden layer,  $f(\ )$  denotes the function of node  $j$  in the hidden layer,  $f(\ )$  usually adopts the Sigmoid function:  $f(x) = 1/(1 + e^{-x})$ .  $x_i^{(k)}$  denotes the input to the modified Elman network,  $i = 1, \dots, M$ . The input consists of three nodes in this work, which corresponds to the throttle position duration signal, respectively;  $y^{(k)}$ , denotes the output from the network, is the expected air fuel ratio signal without the transportation delay.  $x_i^{(k)}$  input datum and  $y^{(k)}$  output datum according to the sampling sequence.  $M, N, L$  denotes the number of the nodes in the input layer, the output layer and the hidden layer, respectively. The number of the nodes in the context layer is equal to that of the hidden layer. Mathematically, the network can be expressed with the following equations:

$$o\_c_j^{(k)} = \beta \cdot o\_c_j^{(k-1)} + net\_c_j^{(k)} \quad j = 1, \dots, L \quad (14)$$

$$net\_h_j^{(k)} = \sum_{i=1}^M w_{1,ij} \cdot x_i^{(k)} + \sum_{i=1}^L w_{3,ij} \cdot o\_c_i^{(k)} \quad j = 1, \dots, L \quad (15)$$

$$o\_h_j^{(k)} = f(net\_h_j^{(k)}) \quad j = 1, \dots, L \quad (16)$$

$$y^{(k)} = \sum_{i=1}^L w_{2,i} \cdot o\_h_i^{(k)} \quad (17)$$

Herein, the input to the context layer at sampling time is the corresponding node output of the hidden layer at sampling time,

$$net\_c_i^{(k)} = o\_h_i^{(k-1)} \quad (18)$$

In this work, the modified Elman network was trained using the gradient descent method. The objective function of the network can be expressed as follows,

$$E = \frac{1}{2} (Y^{(k)} - y^{(k)})^2 \quad (19)$$

is the expected output of the output layer at sampling time, it comes from the output signal of the UEGO sensor.

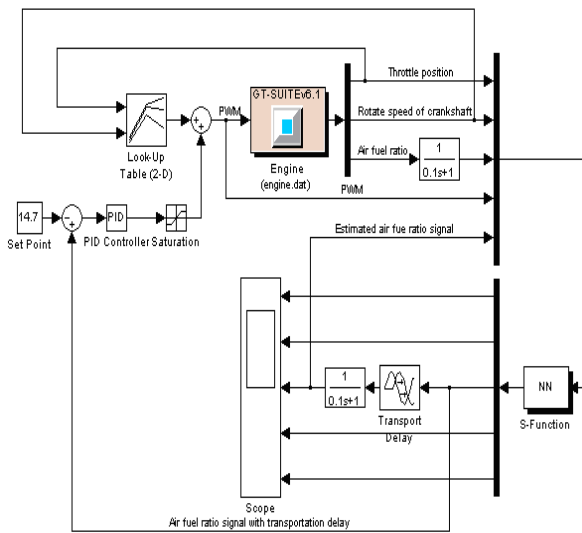


**Figure11. The simulation model of air fuel ratio control based on neural network**

The weight is amended every sampling, and what we have used is the gradient of instantaneous error, which is different from the total gradient of multi-sampling study, so the learning rate of networks should be smaller. In this way their effects will be not so different [13,14].

*B. Air fuel ratio control based on neural network*

The simulation model of air fuel ratio control based on the neural network is illustrated as Figure 11. The output of the UEGO sensor was used to supervise the trained results of the network, so that the air fuel ratio signal without transportation delay can be predicted online. The modified Elman algorithm for predicting the signal without transfer delay was programmed with S-functions. When the throttle changed suddenly, the maladjustment of the air fuel ratio decreased greatly, the controlled error can be kept within the range of  $\pm 3\%$ , illustrated as Figure 12.

**VII. CONCLUSIONS**

The model of a single cylinder electronic controlled engine was set up in this paper by using GT-Power, the simulation model in air fuel ratio control using GT-Power/Simulink was set up as well. On basis of this, the air fuel ratio controlled strategy that combined the modified neural network and the traditional PI algorithm was studied. The results of simulation experiments showed that it is feasible to validate the control strategy by using the simulation model of air fuel ratio control using GT-Power/Simulink. The air fuel ratio transportation delay existing in the gasoline engine causes the bad controlled quality in the transient state. Combined control strategy can achieve the real-time prediction of the air fuel ratio signal without the

transportation delay. The target value of the air fuel ratio can be kept within the range of  $\pm 3\%$  in the transient.

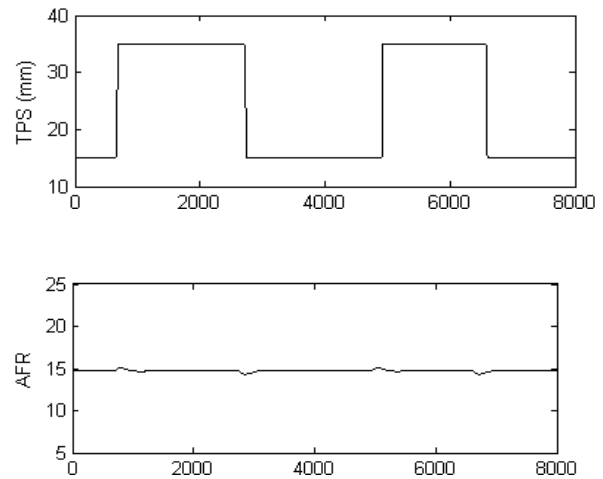


**Figure 12. The controlled results of air fuel ratio based on neural network**

Bench test for the best duty-cycle calibration of LPG EFI under steady condition is conducted in bench testing environment. According to the result can we get the cycle pulse spectrum figure on the relationship among throttle angle- speed-duty-cycle. Also the bench test for the calibration, which tests transmission delay time of air-fuel ratio, is conducted in the transition condition, and from this test can we get the pulse spectrum figure on the relationship among speed-load-air-fuel ratio.

In the simulation and bench test platform these experiments are carried out as follow: air-fuel ratio open-loop experiment of the engine injected by electronically controlled LPG under transition condition, the controlling experiment of PID closed-loop control algorithm for air-fuel ratio under transition condition combined with the pulse spectrum, and the experiment of the closed-loop neurological network algorithm and PID control algorithm on air-fuel ratio under transition condition combined with pulse spectrum.

**REFERENCES**

- [1] Y. H. Tan, S. Mehrdad. Neural-networks-based nonlinear dynamic modeling for automotive engines [J]. Neurocomputing. 2000, 30(2): 129-142.
- [2] Shinichiro Horiuchi, Toshiyuki Tamatsukuri, Shinya Nohtomi. An automotive lateral controller based on generalized predictive control theory, JSAE Review. 2000, 21: 53-59
- [3] Chris Manzie, Marimuthu Palaniswami and Harry Watson. A novel approach to fuel Injection using a radial basis network. IEEE. 1998: 986-991
- [4] Yao Jubiao. Fault diagnosis of Electric-hydraulic servo valves base on road roller[J]. Chinese hydraulics & Pneumatics. 2008, 206(10): 85-87.
- [5] CERCÓS Javier Nevot, CASIN Joseba Quevedo. Air-fuel ratio control of a gasoline engine by means of a recurrent neural network with differentiated input[J]. Integrated Computer-Aided Engineering, 2001(8): 243-255

- [6] Yao Jubiao, Zhou Dasen, Wu Bin. Application on the road test of UA302/H Data Card based on auxiliary [J]. China: Microcomputer Information. 2008, 31: 81-87
- [7] Liu Yabin, Liu Xuétian, et al. Forecast of gas line status at real time based on modified Elman neural network[J]. China: Journal of Systems Engineering, 2003, 18(5): 475-478.
- [8] Yao Jubiao. Research on transient Air Fuel Ratio control of gasoline engines [C]. 2009 International Forum on Information Technology and Applications. 2009, Volume 1: 610-613
- [9] Yao Jubiao, Wu Bin, Zhou Dasen. Simulation Control on transient Air Fuel Ratio of electronic controlled LPG engine Using GT-Power/Simulink[J]. Journal of Beijing University of Technology (Social Sciences Edition). 2009, 35(03)
- [10] Richard K Stobart, Bernard J Challen and Rob Bowyer. Electronic Control-Breedig New Engines. SAE Paper No. 2001-01-0255
- [11] Huang Guanli, Wang Hui, et al. Research on drifting of positioning based on temporal series[J]. China: Computer Engineering and Applications, 2008, 44(31): 94-97
- [12] MANZIE C, PALANISWAM M I, RALPH D, et al. Model predictive control of a fuel injection system with a radial basis function network observer [J]. Journal of Dynamic Systems Measurement and Control. 2002, 124,(4): 648-658.
- [13] Takeshi Takiyamaa, Eisuke Shiomib, Shigeyuki Moritaa. Air - fuel ratio control system using pulse width and amplitude modulation at transient state. JSAE Review. 2001, 22: 537-544
- [14] Andrew Mills. Controlling the sensitivity of optical oxygen sensors. Sensors and Actuators B. 1998, 51: 60-68

**Yao Jubiao**, D.E. in thermal engineering, Beijing University of Technology, China, 2009. Dr. Yao is currently an Associate Professor at Beijing Vocational College of Electronic Science. He leads the teaching departments as dean. He published widely. He has published academic articles in Journal of Beijing University of Technology (Social Sciences Edition), Microcomputer Information and Chinese Hydraulics & Pneumatics etc. His research interests include thermal engineering, electronic auto. Technology and pollution control.

**Jiang Keyu**, Ph.D. in Computer Science, Arizona State University, USA, 2001. Dr. Jiang is currently an Associate Professor at Fort Hays State University where he leads the Information Assurance program within the Informatics Department and National Center of Academic Excellence in Information Assurance (NCAEIA). He published widely. He has published academic articles in Journal of Computing Sciences in Colleges, Journal of Business and Leadership, and Academic Perspective, etc. His research interests include information assurance, distributed system computing and organizational management.

**Yao Chaoyi**, B.E. in civil engineering, Southwest Jiaotong University, China, 2009. He is currently a professional student with master's degree of Southwest Jiaotong University. His research interests include civil engineering, computing and information management.